

**UNIVERSITÀ DEGLI STUDI DI MILANO**

**CORSO DI DOTTORATO IN SCIENZE FARMACOLOGICHE  
BIOMOLECOLARI, SPERIMENTALI E CLINICHE**

**PHD IN PHARMACOLOGICAL BIOMOLECULAR SCIENCES,  
EXPERIMENTAL AND CLINICAL**

**TESI DI DOTTORATO DI RICERCA**

*Upper motor neuron burden in Amyotrophic Lateral Sclerosis:  
clinical and imaging features, and the role of iron metabolism*

SSD: MED/26-Neurologia

**Dott.ssa Enrica Bersano**

**Tutor: Prof. Giuseppe Lauria Pinter**

**Coordinatore: Prof. Giuseppe Danilo Norata**

**A.A. 2022-2023**

## **Riassunto**

**Introduzione.** La Sclerosi Laterale Amiotrofica (SLA) è una patologia rara, a prognosi infausta, in cui la degenerazione del primo e del secondo motoneurone sono coinvolte in modo selettivo. Un elemento di difficoltà nella diagnosi e nel definire una terapia efficace è la considerevole eterogeneità nella presentazione clinica, in assenza di marcatori biologici specifici, dovuta anche ai molteplici meccanismi patogenetici coinvolti nella malattia. In questo progetto di Dottorato è stato preso in considerazione in particolare il metabolismo del ferro, poiché coinvolto in particolare nella degenerazione della via motoria centrale. Studi *post mortem* sui pazienti hanno dimostrato che l'accumulo di ferro intracellulare cerebrale è presente nelle medesime aree corticali che in vivo erano state identificate alla Risonanza Magnetica cerebrale (RMN). In particolare, la tecnica di mappatura di suscettibilità magnetica (QSM) sembra essere un valido strumento per misurare l'accumulo di ferro cerebrale con la RMN. A livello ematico, invece, la ferritina e la transferrina sierica sono noti biomarcatori del metabolismo del ferro nella SLA; mentre l'enzima Glutazione Perossidasi di tipo 4 (GPX4), che svolge un ruolo fondamentale nella regolazione della ferroptosi, è stato studiato attualmente solo nei modelli murini di SLA.

L'**obbiettivo** di questo Progetto di Dottorato è studiare la correlazione tra il danno del primo neurone di moto (UMN), valutato sia clinicamente che con moderne tecniche di neuroimmagine, e i possibili biomarcatori sierici del metabolismo del ferro.

**Metodi.** Sono stati reclutati 68 pazienti, seguiti presso il Centro SLA dell'IRCCS Istituto Neurologico Carlo Besta di Milano, i quali hanno eseguito un prelievo ematico per il dosaggio di ferritina, transferrina e GPX4, e una risonanza magnetica cerebrale con la tecnica QSM. Di questi pazienti sono state raccolte informazioni demografiche e dati clinici sulla gravità di malattia, valutando altresì contestualmente il coinvolgimento del primo neurone di moto attraverso la scala clinica semiquantitativa PUMNS. Inoltre, sono state reclutate 67 persone come controlli sani.

**Analisi Statistiche.** Il test di U Mann Whitney e le correlazioni di Pearson sono state eseguite per studiare la correlazione tra i biomarcatori sierici del metabolismo del ferro e gli indicatori clinici di malattia. Per analizzare gli aspetti radiologici sono state applicate due modalità di studio: per regioni di interesse (ROI) e per morfometria basata sui voxel per l'intero encefalo. Utilizzando lo Spearman test è stata studiata l'associazione tra i valori di QSM estratti dalle sequenze di MRI e i biomarcatori; come parte di questa valutazione, è stata inoltre analizzata la correlazione tra le variabili radiologiche e quelle cliniche. Tutte le analisi sono state verificate per l'effetto dell'età come covariata, e i risultati sono stati ritenuti statisticamente significativi in presenza di un *p value* < 0.05.

**Risultati.** I controlli sani e i pazienti sono risultati omogenei per età e genere. Dal raffronto tra 60 pazienti affetti da SLA e 53 controlli sani della stessa età, è emersa una differenza statisticamente significativa per i livelli di ferritina ( $p = 0.009$ ) e di GPX4 ( $p = 0.001$ ). Analizzando più specificatamente la corte di pazienti SLA risulta che: i livelli di ferritina e transferrina sono inversamente proporzionali tra loro; i livelli di transferrina sono correlati all'indice di massa corporea (BMI); i livelli di ferritina, transferrina e GPX4 non sono correlati né con il genotipo né con gli indicatori di gravità di malattia (quali il punteggio di ALSFRS-R, lo stadio secondo la classificazione di King, la durata di malattia, l'assetto cognitivo o la funzionalità respiratoria). Per contro, una correlazione positiva ( $p < 0.005$ ) è stata riscontrata tra i livelli di GPX4 e il punteggio alla scala di PUMNS, che valuta il coinvolgimento clinico del primo motoneurone. Analizzando i dati di RMN dei pazienti e dei controlli sono stati riscontrati differenti valori di suscettibilità magnetica (QSM) in specifiche aree motorie cerebrali (putamen bilateralmente, VIII lobulo cerebellare di sinistra cerebellare, lobuli IV-V di destra e I cerebellare con un  $p < 0.001$ ). Confrontando i pazienti SLA con un sottogruppo dei controlli sani, che avevano eseguito sia la RMN che il prelievo di sangue, non si è rilevata alcuna differenza tra i livelli di GPX4 e il valore di QSM. Tuttavia, se si escludono i soggetti con valori di GPX4 anomali, si evidenzia una correlazione positiva ( $p < 0.001$ ) nella regione destra della corteccia motoria primaria (M1). Analizzando il solo gruppo di pazienti SLA, con analisi di regressione lineare sono state messe in evidenza correlazioni positive tra il QSM ( $p$

< 0.05); e GPX4 nell'area M1 di sinistra; e transferrina nell' area ventrale e dorsale premotoria e nella area motoria supplementare (SMA); e ferritina nei lobuli IV-V cerebellari di sinistra, nel nucleo caudato, nel talamo e nella SMA di destra. Considerando i parametri clinici invece, non vi è una correlazione con i punteggi PUMNS, fatta eccezione per il confronto tra il punteggio che riguarda il solo distretto degli arti superiori e il valore di QSM nella sole regioni della preSMA e SMA dell'emisfero destro ( $p < 0.04$ ). Tuttavia, se si analizza il grado di coinvolgimento del primo motoneurone secondo il fenotipo, si trova una correlazione positiva in M1 ( $p < 0.004$ ) e una correlazione negativa nei lobuli cerebellari IV-V di sinistra ( $p < 0.04$ ).

**Discussione.** Dal confronto con controlli sani di pari età, i risultati confermano come i pazienti affetti da SLA siano caratterizzati da maggiori livelli di ferritina, sebbene non vi sia alcuna specifica correlazione con i fenotipi di malattia. Tuttavia, il presente lavoro è il primo che dimostra che anche i livelli di GPX4 sono statisticamente più elevati nei pazienti rispetto alla popolazione sana. Inoltre, analizzando la distribuzione dei livelli di GXP4 nei pazienti affetti da SLA non sono state riscontrate correlazioni con le caratteristiche cliniche della malattia ad eccezione di ciò che riguarda il coinvolgimento del primo neurone di moto, valutato sia clinicamente che radiologicamente. Coerentemente con quanto riportato in letteratura, l'analisi delle caratteristiche radiologiche in RMN ha confermato che valori più elevati di QSM si associano a una maggiore compromissione della via motoria centrale, in particolare nella regione M1 di sinistra. Inoltre, il presente studio è il primo, a nostra conoscenza, ad indagare una possibile relazione tra i livelli sierici dei marcatori del metabolismo del ferro e l'accumulo cerebrale di ferro valutabile con la RMN, mostrando in particolare come vi sia una correlazione positiva tra i valori di GPX4 e di QSM nell'area M1.

**Conclusioni.** Il presente studio ha indagato, nei pazienti affetti da SLA, la correlazione tra la compromissione del primo motoneurone, valutato sia clinicamente che con i valori di QSM nelle diverse aree corticali cerebrali, e i biomarcatori sierici del metabolismo del ferro. I risultati della presente ricerca

suggeriscono che il GPX4 possa essere un biomarcatore utile nella differenziazione fenotipica e nella predizione della progressione di malattia.

## **Abstract**

**Background.** Amyotrophic Lateral Sclerosis (ALS) is a rare fatal neurodegenerative disease selectively affecting upper and lower motor neuron system, with a heterogeneity of phenotypes which cannot currently be distinguished by specific biomarkers. The present research focuses on iron metabolism as one of the pathogenetic mechanisms of ALS. Ferritin and transferrin are well-known biomarkers of iron metabolism in ALS, while the role of Glutathione Peroxidase 4, one of the main factors of ferroptosis, is still unknown as it has only been explored in ALS mice. In vivo, iron accumulation in brain is detectable by Quantitative Susceptibility Mapping (QSM) technique on Magnetic Resonance Imaging (MRI) and correlates with the upper motor neuron damage.

The **aim** of the project is to investigate the correlation between upper motor neuron (UMN) impairment detected by clinical and neuroimaging techniques and serum biomarkers of iron metabolism.

**Methods.** 68 ALS patients, followed at ALS Center of “IRCCS Istituto Neurologico Carlo Besta” of Milan, were recruited for this study, collecting demographic features and clinical data on severity of disease, and the involvement of Upper motor neuron involvement detected with PUMNS scale at time of visit. 60 also provided blood samples to dose ferritin, transferrin and GPX4 enzyme in serum, and 52 additionally performed a brain MRI with QSM value. 67 Healthy Controls (HC) were also recruited.

**Statistical analyses.** To assess whether serum biomarkers can be considered as indicator of disease, it was first explored the possible correlation between iron serum biomarkers and clinical data with U Mann Whitney test and Pearson correlation, then it was investigated the association of biomarkers with radiological features (QSM values) by applying Spearman test, also testing the correlation between radiological and clinical features.

**Results.** ALS and HC were homogeneous for age and gender. A statistically significant difference of ferritin ( $p = 0.009$ ) and GPX4 ( $p = 0.001$ ) levels was found

when comparing 60 ALS with 53 age-matched HC. In the ALS cohort: ferritin was inversely related to transferrin; transferrin correlated with the Body Mass Index; ferritin, transferrin and GPX4 had no correlation with genetic assessment or severity of disease. Instead, a positive correlation ( $p < 0.005$ ) was found between GPX4 and PUMNS score. Regarding the evaluations of QSM values on brain MRI, variations of magnetic susceptibility in ALS patients as compared to HC were found in specific motor areas of brain ( $p < 0.001$ ). By comparing MND with the subgroup of HC who both underwent MRI and blood withdrawal, no correlation was found between GPX4 and QSM values. However, when excluding subjects with outlier values of GPX4, a positive correlation was revealed in right M1 region ( $p < 0.001$ ). Regression analysis across ALS group showed positive correlations ( $p < 0.05$ ): with GPX4 in primary motor cortex area on left side (M1); with transferrin in ventral and dorsal premotor cortex and in supplementary motor area (SMA); and with ferritin in left lobules IV-V cerebellum, caudato, thalamo and in right SMA. Instead, no significant correlation was found with clinical score of upper motor neuron (UMN) burden, except for sub-score about upper district in right preSMA and right SMA ( $p < 0.04$ ). By performing a trend analysis with rank of UMN involvement, a positive trend in left M1 ( $p < 0.004$ ) and a negative trend in left lobules IV-V of cerebellum ( $p < 0.04$ ) were identified.

**Discussion.** Compared to age-matched HC, there is a higher level of serum ferritin in patients, but it does not correlate with any specific phenotype. Instead, the present research first shows that serum levels of GPX4 are statistically higher in ALS than HC. Moreover, the analyses of GPX4 trend in ALS cohort did not find any correlation with features of disease, with the exception of the UMN burden. Regarding MRI features, in M1 region higher levels of QSM are associated with the degree of UMN involvement, and with GPX4 levels.

**Conclusion.** The findings of the present research suggest that GPX4 can be a useful biomarker of UMN involvement in ALS patients, linked to iron brain accumulation evaluated with QSM technique, with a potential impact on phenotypes differentiation and disease progression prediction.

# **Upper motor neuron burden in Amyotrophic Lateral Sclerosis: clinical and imaging features, and the role of iron metabolism**

## **Introduction**

Amyotrophic Lateral Sclerosis (ALS) is a rare fatal neurodegenerative disease that predominantly affects the upper and lower motor neuron system. The heterogeneity of phenotypes, particularly in early stages of disease, and the different disease progression suggest the involvement of several pathogenic mechanisms of disease. Currently, there is no high-quality biomarkers for the diagnosis of specific phenotypes, while the complexity of the genotype-phenotype relationship makes difficult predicting disease progression. Among several pathogenic mechanisms of ALS, the present research focuses on iron metabolism, as iron dyshomeostasis is involved in ageing processes and several neurodegenerative disorder. The aim of the project is to investigate the correlation between upper motor neuron (UMN) impairment detected by clinical and neuroimaging techniques and serum biomarkers of iron metabolism. The identification of serum proteins and radiological features as markers of this specific phenotype of the disease could be useful in the clinical assessment of patients and the design of clinical trials.

## **Background**

### ***Motor Neuron Disease***

Motor Neuron Disease (MND), also known as Amyotrophic Lateral Sclerosis (ALS), is a fatal neurodegenerative disorder characterised by progressive painless muscles weakness due to motor neuron death in the brain, brainstem, and spinal cord.<sup>1</sup> ALS has historically been considered as a pure, uniform, and exclusive motor syndrome, a view overcome by strong evidence of multisystemic involvement, particularly of cognitive and/or behavioural impairment, ranging from frontotemporal dementia (FTD) to milder forms of executive or dysexecutive dysfunctions and estimated to affect about 30-50% of patients. Also, motor clinical presentation is heterogenous with regards to site of onset (bulbar region, limbs, thoracic involvement), regional



spreading of symptoms, and the distribution of upper (UMN) and lower (LMN) motor signs; in particular, the latter can lead to classic forms of ALS, or range from pure/predominant UMN to pure/predominant LMN disease forms. Different motor clinical presentations influence disease progression, diagnostic delay, and prognosis. In fact, death from ALS generally occurs from respiratory failure within two to four years from diagnosis, though more slowly progressing forms, at the end of MND spectrum, occur in about 15-20% of patients.

According to international guidelines<sup>2,3</sup>, the diagnosis of MND predominantly relies on the interpretation of clinical signs and neurophysiological findings, while laboratory and neuroradiological examinations are employed to rule out other causes. Currently, there is no high-quality biomarker for diagnosis and prognosis; however, research on biochemical, imaging and neurophysiology techniques is growing.<sup>4</sup> The lack of biomarkers hinders the possibility to distinguish phenotypes and to predict disease progression. In about 10% of patients, the family history suggests an autosomal dominant inheritance pattern (familial ALS, fALS), while in the remaining 90% no affected family members are reported (sporadic ALS, sALS). Nevertheless, fALS and sALS show similar clinical and neuropathological features.<sup>5</sup> In 1993, the first mutation causing fALS was found in *Cu/Zn Superoxide dismutase 1 (SOD1)* gene; since then, more than 50 genes increasing the risk of developing disease, or modifying the ALS phenotype, have been identified. For an individual ALS with an affected first degree relative, the pre-test probability of a positive genetic test is currently about 70%; instead, for those with negative family history (sALS), the probability is about 10%. In addition to *SOD1*, the other most common genetic causes are hexanucleotide expansion in chromosome 9 open reading frame 72 (*C9orf72*), mutations in TAR DNA-binding protein 43 (*TARDBP*), fused in sarcoma (*FUS*) and TANK-binding kinase 1 (*TBK1*). Though most mutations converge on a typical ALS phenotype, there are important prognostic implications for certain mutant genes linked to unique features, e.g., *OPTN* mutations for ALS type 2. A gene therapy is now available for ALS patients with *SOD1* mutations and is undergoing clinical trial for patients with *FUS* and *C9ORF72* mutations.<sup>6</sup>

Data collected from ALS patient's consortium show the highlight complexity of the disease's genotype-phenotype relationship and suggest that heterogeneity of disease is underpinned by several pathogenic mechanisms.<sup>5</sup> The most relevant dysfunctions are: alterations in nucleocytoplasmic transport of RNA molecules and binding proteins; altered RNA metabolism; impaired proteostasis with accumulations of aggregating proteins (*TDP-43*, *FUS*, *SOD1*); impaired DNA binding and repairing; mitochondrial dysfunction and oxidative stress; oligodendrocyte degeneration; neuroinflammation; defective axonal and vesicular transport; and excitotoxicity.<sup>5</sup>

### ***The role of iron in MND***

The present research focuses on iron metabolism, one of the several pathogenic dysfunctions of MND. Iron dyshomeostasis is involved in ageing processes and in neurodegenerative disorders,<sup>7</sup> such as Alzheimer and Parkinson diseases. Iron is a vital cofactor in many brain metabolic processes, including oxygen transportation, DNA and myelin synthesis, mitochondrial respiration, and neurotransmitter synthesis and metabolism.

In *SOD1* transgenic mice and ALS cell models, dysfunctional *SOD1* results in imbalance between free radicals and ions, ultimately culminating in increased cellular oxidative stress and releasing of iron from iron containing protein. Moreover, the double transgenic mice for *SOD1* and hemochromatosis gene (*HFE*) had a shorter survival and an accelerated disease progression<sup>8</sup>. In human, although some studies suggested the p.H63D polymorphism of *HFE* as a risk factor for ALS<sup>8,9</sup>, two meta-analyses of literature rejected such assumption<sup>10,11</sup>. No effect of *HFE* status was found in an Italian cohort of patients carrying *C9ORF72*, *TARDBP*, and *FUS* mutations; the few *SOD1* patients with p.His63Asp CG or GG polymorphism were also associated with a longer survival<sup>12</sup>.

In post-mortem histopathologic analysis of brains of ALS patient it was revealed an abundancy of cells containing intracellular iron, also in microglia, and of extracellular iron deposits in motor cortex, caudate and subthalamic nuclei<sup>13</sup>. Studies conducted in the 1990s have observed iron accumulation in the spinal cord

and cerebrospinal fluid of patients<sup>14</sup>. Iron chelators, such as salicylaldehyde isonicotinoyl hydrazone, deferoxamine and deferiprone, have been employed in murine model and pilot clinical trials<sup>15-17</sup>. These studies confirm the role of iron homeostasis and excessive iron accumulation in central nervous system in development and disease progression of ALS.

Ferritin and transferrin are well-known biomarkers for iron metabolism in MND. Serum ferritin levels in MND patient, regardless of genetic assessment, were found to be significantly higher and transferrin levels lower compared to healthy controls, while no statistical difference in iron levels between MND patients and controls was reported<sup>18</sup>. Additionally, higher serum ferritin levels have been associated with shorter survival<sup>19</sup>, but are not related to any specific phenotype.

### ***Magnetic Resonance iron imaging in MND***

The diagnostic work up of patients suspected of suffering from MND includes magnetic resonance imaging (MRI) of brain and spinal cord to rule out structural abnormalities (e.g., vascular lesions, multiple sclerosis, tumors, radiculopathy, myelopathy). Neuroimaging in MND is sensitive for detecting extra-motor brain involvement, particularly in frontotemporal cortical regions, and is also an ideal tool for measuring upper motor neuron impairment in a non-invasive way. Evidence suggests that neuroimaging can be applied to correctly diagnose MND, and stratify patients into different phenotypes, stages, and prognostic categories<sup>20</sup>. MRI has the powerful ability to generate a series of image contrasts that map the scale distribution of iron in vivo in the human brain<sup>21</sup>.

Although iron accumulation in brain increases as part of the normal aging process, the post-mortem finding from MND patients showed that the increased iron accumulation in microglial cells of the deep layers of motor cortex corresponds to the same areas of MRI signal changes<sup>22</sup>. According to the standard clinical parameters, iron rich tissues appear isointense in T1-weighted (T1W), and hypointense in T2-weighted (T2W) as well as T2\*W gradient-echo sequences (T2\*W2). However, signal alteration in fluid-attenuated inversion recovery (FLAIR)

images are inconsistently present in MND imaging studies, therefore FLAIR sequence does not appear to be specific of MND. Susceptibility Weighted Imaging (SWI), instead, is a technique that uses a high-resolution three-dimensional gradient echo sequence with full flow compensation and improved sensitivity in detection of ferric iron compared to T2\*W2. SWI showed iron accumulation in precentral cortices<sup>23-25</sup> and in white matter tracks<sup>26</sup> when comparing MND patients with control subjects. Nevertheless, SWI presents some intrinsic technical limitations (blooming and air tissue artifacts) and does not allow quantitative measurement of magnetic susceptibility.

To address these shortcomings, Quantitative Susceptibility Mapping (QSM) technique can be used as a surrogate measurement of quantitative iron concentration in the brain based on magnetic susceptibility in vivo. Recently, both the development of new QSM reconstruction algorithms and their use on neurodegenerative diseases, from Alzheimer dementia to Parkinson disease, have greatly increased. Several studies show the potential role of QSM as a diagnostic tool in ALS. In whole brain QSM approach, increased iron was revealed in the motor cortex, substantia nigra, globus pallidus, and red nucleus<sup>27</sup>: significant differences in QSM measures in the motor cortex have been reported in ALS compared to healthy controls<sup>28</sup>, and among ALS patients according to onset disease (lumbar versus cervical<sup>29</sup> and bulbar onset<sup>30</sup>); although no change in QSM was reported in a 6-month follow up study<sup>31</sup>, the magnetic susceptibility in precentral cortex diversified according to MND phenotype, particularly reflecting the prevalence of upper or lower motor neuron signs<sup>32</sup>. Based on these studies, it was suggested that QSM could be considered a biomarker in iron-related MND subtypes and could be useful for specific clinical trials.

#### ***Glutathione peroxidase 4 (GPX4) and its role in ferroptosis***

Glutathione peroxidases (GPXs) constitutes an interesting family of oxidoreductases observed in all living organisms. Eight isoforms of GPX enzymes have been discovered in all tissues, and their redox properties in balancing oxidative homeostasis in cells as well as the post translational modification of proteins

signalling pathways are currently well established<sup>33</sup>. More specifically, Glutathione peroxidase 4 (GPX4) is the only type of GPX to be ubiquitously expressed, and to be capable of reducing large and complex lipid hydroperoxides and cholesterol, even when they are embedded in the biological membrane; GPX4 is therefore essential for life, from embryonic development to health maintenance in adult animals.

A feature of ferroptosis is the accumulation of phospholipid hydroperoxides in the presence of catalytically active iron. This process is inhibited by the system Cysteine/GSH/GPX4 regulatory pathway. GPX4 uses glutathione as an electron donor to reduce highly toxic lipid hydroperoxides in membranes to less toxic lipid alcohols. Depletion of GPX4 causes an increase in lipid peroxides that damages the cell membrane, and leads to ferroptotic cell death<sup>34</sup>.

GPX4 is an emerging topic of pharmacological research, and it is already a target for precision therapy for Sedaghatian-type spondylometaphyseal dysplasia (SSMD) – a rare genetic disorder<sup>33</sup>.

GPX4 is involved in the degeneration of cortical and hippocampal neurons, and interneurons in mice<sup>35</sup>. GPX4-NIKO mouse is a versatile model for testing interventions targeting ferroptotic death of spinal motor neurons *in vivo*<sup>36</sup>. Ablation of GPX4 in neurons of adult mice triggered a rapid degeneration of spinal motor neurons<sup>35</sup>, resulting in a savage paralysis, while the symptomatic *SOD1G93A* mice had a deficiency of GPX4 in spinal cord tissues and a reduced level of GSH<sup>37</sup>.

While GSH depletion is a known feature of affected central nervous system tissues of ALS patients, a deficiency of GPX4 protein in ALS patients has been reported in a few studies analysing mean GPX4 protein levels in lumbar spinal cord tissues versus controls<sup>37,38,39</sup>. Wang et al demonstrated that GPX4 depletion was common to both familial and sporadic ALS patients and three distinct genetic mouse models of ALS. The authors noted that GPX4 downregulation is not a consequence of neurodegeneration, as GPX4 levels fell early in spinal cords and cortices of *SOD1G93A* mice, preceding symptoms and motor neuron loss<sup>38</sup>. The intrathecal injection of neuron-targeted GPX4 and the treatment of phospholipid peroxidation

inhibitor, ferrostatin 1, significantly attenuates motor dysfunction in ALS mice, and suggests a possible role of GPX4 in maintaining brain immune homeostasis<sup>39</sup>.

Based on the analysis of GPX4 gene expression in both ALS patients and mice, Tu et al. proposed the applicability of a GPX4-related treatment, as neuron-targeted GPX4-AAV delivery prohibited phospholipid peroxidation and improved the viability of motor neurons.<sup>39</sup>

In addition, one drug tested in ALS disease, *Edaravone* (3-methyl-1-phenyl-2-pyrazolin-5-one), is involved in ferroptosis and GPX4 regulation. *Edaravone* is an excellent free radical scavenger originally developed for the treatment of acute ischemic stroke due to its neuroprotective role in vascular endothelium and glial cells damages<sup>40,41</sup>. Later, *Edaravone* was also developed for the treatment of MND based on its anti-oxidative and intracellular lipid stabilising effects that prevent ferroptosis<sup>42,43</sup>. Furthermore, the anti-ferroptosis role of *Edaravone* via GPX4 pathway is involved in depression, and the GPX4 knockdown removed the effect of *Edaravone* treatment<sup>44</sup>. In the acute phase of spinal cord injury, *Edaravone* reduced neuronal cell death and neuroinflammation by acting on ferroptosis negative regulators such as GPX4, and by downregulating pro-ferroptosis factors<sup>45</sup>.

### **Aim of PhD project**

Hypothesis: if QSM value at MRI can detect iron accumulation which reflects upper motor involvement in MND, is the alteration of iron typical of upper motor neuron dominant phenotype of MND? Could ferritin, transferrin and GPX4 protein in serum be a useful biomarker of upper motor neuron alteration?

The aim of the project is to investigate the correlation between upper motor neuron (UMN) impairment assessed by clinical evaluation and neuroimaging techniques, and serum biomarkers of iron metabolism.

### **Methods**

The study involved 68 ALS patients followed at the Fondazione IRCCS Istituto Neurologico “Carlo Besta” in Milan, and 67 healthy controls. The patients were enrolled with a written informed consent within *TRANSALS* and *INTERSLA* projects, approved by Ethic Committee.

### ***MND Patients***

All patients recruited for the study were affected by MND diagnosed according to El Escorial revised diagnostic criteria.<sup>46</sup> The following data have been collected: demographic data, age and site of onset disease, age of diagnosis, regions involved at time of visit (bulbar, upper and lower limbs), cognitive and behavioural features according to Strong’s criteria<sup>47</sup>, disease severity assessed by ALS Functional Rating Scale revised (ALSF<sub>RS</sub>-R)<sup>48</sup>, pulmonary function tested by the forced vital capacity<sup>49</sup> (FVC%) at spirometry, Body Mass Index (BMI) calculated by a nutritionist, stage of disease at time of visit evaluated according to King’s Clinical Staging System<sup>50</sup>. The genotype has been determined by analysing a panel of 10 genes (*SOD1*, *FUS-TLS*, *C9ORF72*, *TARDBP*, *PFN1*, *VCP*, *TUBA4A*, *OPTN*, *SQSTM1*, *UBQLN2*) as routinely performed at the MND Center. The phenotype was defined by relying on clinical evaluations and neurophysiological assessments, and classified according to the following categories: bulbar, spinal with predominant upper motor neuron damage (UMN), spinal with predominant lower motor neuron damage (LMN), and spinal (with no prevalence of upper or lower motor neuron impairment); patients diagnosed with Primary Lateral Sclerosis (PLS), a part of spectrum of MND defined by the presence of symptoms of progressive UMN dysfunction for at least 2 years in absence of significant active LMN degeneration 2–4 years from symptom onset<sup>51</sup>, were also included as a fifth category. At time of visit, all patients underwent an assessment of the involvement of upper motor neuron damage, based on a clinical examination using the Penn Upper Motor Neuron Score (PUMNS), i.e. a semiquantitative scale ranging from 0 to 32 (0-4 for the bulbar segment, 0-7 for each limb) with higher scores associated to greater UMN burden<sup>52</sup> ([Table 1](#)).

In the PUMNS scale, one point is given for each of the following abnormal tendon reflexes: Triceps, Biceps, Patellar and Achilles; one additional point is added in each

limb if clonus is present; one point is given for each Hoffman’s sign, Babinski sign, presence of a jaw jerk, presence of a facial reflex, and presence of a palmomental sign; one point is given for pseudobulbar affect, using the CNS-Lability scale  $\geq 13$  as a cutoff. The Ashworth scale has been used to grade the tone in each limb: one point was given for an Ashworth scale grade of 2–3, and 2 points for an Ashworth scale grade of 4–5.

**Table 1: Penn Upper Motor Neuron Score (PUMNS)**

Penn Upper Motor Neuron Score (PUMNS)		
Bulbar Subscore (0-4)		
	Score	
Jaw-jerk reflex (0-1)		
Facial reflex (0-1)		
Palmomental sign (0-1)		
Score $\geq 13$ on CNS-Lability Scale (0-1)		
Upper Extremity Subscore (0-7, bilateral)		
	Right	Left
Increased triceps reflex (0-1)		
Increased biceps reflex (0-1)		
Present finger flexor reflex (0-1)		
Hoffman’s sign (0-1)		
Clonus (anywhere in limb) (0-1)		
Additional points for spasticity (0-2):		
Ashworth 1 (normal tone): 0 points		
Ashworth 2-3: 1 point		
Ashworth 4-5: 2 points		
Lower Extremity Subscore (0-7, bilateral)		
	Right	Left
Increased patellar reflex (0-1)		
Crossed adduction (0-1)		
Increased ankle reflex (0-1)		
Babinski’s sign (0-1)		
Clonus (anywhere in limb) (0-1)		
Additional points for spasticity (0-2):		
Ashworth 1 (normal tone): 0 points		
Ashworth 2-3: 1 point		
Ashworth 4-5: 2 points		
	<b>Total (0-32):</b>	

*The Penn Upper Motor Neuron Score (PUMNS) is a semiquantitative scale, ranging from 0 to 32, (0-4 for the bulbar segment, 0-7 for each limb) with higher scores associated to greater UMN burden.*



Since the study concerns iron metabolism, certain aspects have been considered as exclusion criteria; these include severe hepatic disorders and intestinal malabsorption diseases, iron deficiency anaemia and haematological alterations, special diet as vegan diet, fever or signs of acute inflammation, and concomitant psychiatric disorders. Within 1 month from the visit, the patients were given a blood sample and a brain MRI.

### ***Blood samples***

For analysing serum iron biomarker, venous blood samples (5 ml) were taken at time of visit and centrifuged at 3,000 x g for 15 min to collect the supernatant serum. Ferritin (ng/ml) and transferrin (mg/dl) were assessed with Immunology Analyser as routinely measured at Laboratory Department of Istituto Neurologico “Carlo Besta”. Levels of GPX4 (ng/ml) was dosed with Human Glutathione Peroxidase 4 enzyme-linked immunosorbent assay (ELISA KIT, Nanhu Dist, Jiaying, China).

### ***Brain MRI protocol***

MRI data were acquired on Philips scanner equipped with a 32-channel head coils. MRI protocol includes 3D TFE T1-weighted sequence (160 sagittal slices, TR = 1640 ms, TE = 2 ms, FOV = 256 x 256 mm<sup>2</sup>, no gap, voxel size = 1 x 1 x 1 mm<sup>3</sup>, flip angle = 12°) and a multi-echo gradient-echo sequence for QSM quantification. Two different multi-echo gradient-echo sequences were used [version 1: 140 true-transversal slices, field of view (FOV) = 240 x 180 mm<sup>2</sup>, voxel size = 0.5 x 0.5 mm<sup>2</sup>, slice thickness = 1 mm, flip angle = 17°, number of echoes = 7, first TE = 4.5 ms, ΔTE = 5 ms, TR = 40 ms; version 2<sup>53</sup>: 140 true-transversal slices, FOV = 224 x 224 mm<sup>2</sup>, voxel size = 1 x 1 mm<sup>2</sup>, slice thickness = 1 mm, flip angle = 18°, number of echoes = 7, first TE = 5.4 ms, ΔTE = 5.2 ms, TR = 40ms]. Both sequences were acquired within a single MRI scan in a sub-sample of 8 healthy controls to ensure that no significant differences occurred in the QSM quantification in ROIs between the sequences (Wilcoxon test p

> 0.05). Analyses were performed using STI suite toolbox<sup>1</sup>, running in MATLAB 2023a. Patients with severe cerebrovascular encephalopathy were excluded.

The following QSM reconstruction steps were applied to magnitude and phase images. As first step, a bias field inhomogeneity correction using N4-ITK ANTs with default parameters was applied to magnitude images. A brain mask for background phase removal step was obtained from the magnitude image of the echo close to TE = 30 ms (6th echo) using an in-house Matlab script. An optimal threshold of 30% of maximum intensity value was set for all subjects. Possible hole in the mask were filled along transversal and coronal planes (imfill function, Matlab). Each mask was visually inspected before the subsequent steps. The mask evaluation criteria were the inclusion of whole brain and brainstem and the absence of holes and part of the skull. In STI suite, phase unwrapping was performed on phase images at each echo time using a Laplacian-based phase unwrapping to obtain an estimation of field map. Background field removal was obtained on field map applying a variable-kernel sophisticated harmonic artefact reduction for phase data (V-SHARP, varying spherical kernel size up to 25mm)<sup>54</sup> and a sparse linear equation and least-squares-algorithm-based method (iLSQR) was applied, using a zero-padding around the brain of 6 mm. QSM reconstruction map was normalized to the MNI atlas space using ANTs<sup>55</sup>. All QSM normalized maps were smoothed by 6 mm full width at half maximum (FWHM).

### ***Healthy controls***

Age-matched Healthy Controls (HC) were recruited in 2 phases. A first group of HC included 43 underwent blood withdrawal to dose ferritin, transferrin and GPX4 enzyme. A second group of 24 subjects underwent brain MRI with an extensive protocol, including sequences of QSM; 10 of them underwent also blood withdrawal at the same time of MRI to dose GPX4. All subjects underwent clinical interview to rule out severe hepatic disorders and intestinal malabsorption diseases, iron

---

<sup>1</sup> <https://people.eecs.berkeley.edu/~chunlei.liu/software.html>

deficiency anemia and haematological alterations, special diet as vegan diet, fever or signs of acute inflammation and concomitant psychiatric disorders or neurodegenerative disease. Written informed consent was obtained from each participant prior to their inclusion in the study. For the purpose of the present study, HC have been grouped according to the following criteria: those who only performed brain MRI (“HCimaging”, 24 people); those who only performed a blood sample for iron biomarkers (“HCserum”, 53 people); and those who performed both MRI and blood sample (“HCis”, 10 people).

### **Statistical analyses**

Difference was considered to be significant at  $p < 0.05$ . Data were analysed using the statistical spreadsheets Jam-ovi v 1.8.1<sup>2</sup>. Normal distribution of data was determined using the Shapiro Wilk test for GPX4, ferritin and transferrin values. Results are expressed as the mean  $\pm$  standard deviation.

MND vs HC. Age and gender differences were assessed between patients and HC (two samples t-test  $p > 0.05$ ; fisher’s exact test  $p > 0.05$ ). Unpaired t-test and U Mann Whitney test were carried out to detect differences in GPX4, ferritin and transferrin levels between MND group and HCserum.

Pearson correlation was addressed to explore the association between GPX4, ferritin and transferrin with demographic data and indicators of disease (ALSFRS-R, King’s scale, FVC, BMI, PUMNS score total, sub-score of PUMNS in upper, lower and bulbar districts, and duration of disease). While to examine correlation cognitive assessment, cognitive and phenotype One-way ANOVA test was used. All analyses were also checked for the effect of years of age, as covariate.

Regarding the study of MRI features, two analyses were performed: analysis by regions of interest (ROIs) and whole brain voxel-based analysis. The following ROIs

---

<sup>2</sup> <https://www.jamovi.org>

were considered for the motor system (Figure 1). Bilateral regions of caudate nucleus (Caudato), putamen (Putam), pallidum (Pal), thalamus (thalamo), cerebellum lobules IV-VI, VIIIA, VIIIB, obtained from Harvard-Oxford atlas<sup>56</sup> as well as primary motor cortex (M1), dorsal premotor cortex (PMd), ventral premotor cortex (PMv), supplementary motor area (SMA) proper, pre-supplementary motor area (preSMA) and primary somatosensory cortex (S1), obtained from Human Motor Area Template (HMAT)<sup>57</sup>. Regions of motor cerebellum were selected according to the known cerebellar somatotopy<sup>58,59</sup>. For each one of these regions, a binary mask was obtained using FSL. For each ROIs, the mean susceptibility value was extracted. Possible subject outliers were identified (mean value greater than 3 standard deviations of the whole sample in at least 4 regions of interest). Spearman correlation analyses were performed between susceptibility values in the ROIs and the GPX4, ferritin and transferrin values, separately. To assess the correspondence between UMN and LMN involvement, the following analyses were conducted. Firstly, a Spearman correlation analysis was carried out between susceptibility values in the ROIs and the UPMNS scale along with its subscales (Upper, Lower). Secondly, patients were grouped based on an increasing rank of UMN involvement: spinal LMN dominant=1; spinal =2; spinal UMN dominant and PLS=3. Bulbar ALS patients were excluded from the ranking. For each ROI, in order to assess whether there was a trend for decreasing/increasing susceptibility values at the increasing rank of UMN involvement, the Jonckheere-Terpstra test ( $p < 0.05$ ) was applied for ordinal differences between the groups according to rank. Statistical analyses were done using R version 4.3.

Voxel-based analysis was performed in SPM in voxels belonging to motor ROIs. The two-sample t-test was used to compare patients and HCimaging. Spearman correlation analyses were performed between susceptibility values and the GPX4 compared MND group and HCis. Moreover, two voxel-wise regression analysis across all patients with GPX4, transferrin and ferritin values as our primary regressor of interest, respectively, were performed. The results were considered significant using a threshold value for voxels of  $p < 0.005$  with cluster size  $p < 0.05$ .

## Results

The cohort of 68 patients was representative of MND patients by age at onset, gender, and distribution of phenotype. The recruitment was performed at time of diagnosis, and the median of duration of illness was of 18 months (3-83 months). In [Table 2](#), demographic and clinical data of MND patients are reported. For 5 patients the blood serum was unusable for iron biomarker dosing, while 16 patients have been excluded from the radiology assessment analysis due to the presence of artefacts or severe vascular encephalopathy that could bias the QSM value.

**Table 2: Data of MND patients**

	MND patients		
	No.	Range	Mean (SD)
<b>Demographical data</b>			
Age at visit (yrs)	68	39 - 88	61 (11)
Gender (M/F)	34 / 34		
<b>Laboratory test</b>			
Transferrin (mmg/dL)	60	148 - 375	235 (44)
Ferritin (mg/mL)	60	5,63 - 926,51	193 (182)
GPX4 (ng/ml)	63	0,55 - 17,29	3,91 (2,44)
<b>Clinical data</b>			
Phenotype (bulbar / spinal / LMN / PLS / UMN)	12 / 19 / 23 / 3 / 11		
Genotype (neg / c9orf72 / SOD1 / FUS)	56 / 7 / 3 / 2		
Cognitive status (ALScn / ALSbi / ALSci / ALScbi / ALS-FTD)	34 / 6 / 18 / 5 / 4		
King's Clinical Stage (1 / 2 / 3 / 4)	27 / 21 / 19 / 1		
Motor disability (ALSFRS-R)	68	29 - 47	42
Age at onset	68	38 - 88	60
Disease duration (months)	68	3 - 83	18
PUMNS	68	0 - 26	8
BMI	65	18 - 33	24
FVC (%)	63	0% - 157%	99%

MND and HC were homogeneous for demographic features (age and gender) (Table 3).

**Table 3: MND and HC demographic features**

	MND patients						Healthy Controls									Group differences MND / HC
	Total			with QSM value			HCserum			HCis			HCimaging			
	No.	Range	Mean (SD)	No.	Range	Mean (SD)	No.	Range	Mean (SD)	No.	Range	Mean (SD)	No.	Range	Mean (SD)	
<b>Demographical data</b>																
Age at visit (yrs)	68	39 - 88	61 (11)	52	39 - 88	61 (12)	53	42 - 80	61 (11)	10	44 - 77	67 (10)	24	33 - 77	56 (13)	p = 0,971
Gender (M/F)	34 / 34			23 / 29			27 / 26			5 / 5			8 / 16			Z = 0,918
<b>Laboratory test</b>																
Transferrin (mmg/dL)	60	148 - 375	235 (44)				45	173 - 383	247							p = 0,108
Ferritin (mg/mL)	60	5.63 - 926,51	193 (182)				45	7,52 - 380,03	109,63							p = 0,009
GPX4 (ng/ml)	63	0,55 - 17,29	3,91 (2,44)				53	0 - 12,85	3,06							p = 0,001

To assess whether serum biomarkers can be considered as indicator of disease, a twofold analysis was performed. As a first step, it was explored the possible correlation between iron serum biomarkers and clinical data. As a further step of analysis, it was investigated the association of biomarkers with radiological features, namely QSM values extracted from MRI sequences; as part of such assessment, the correlation between radiological and clinical features was also tested.

***Correlation between iron serum biomarkers and clinical data***

A comparison was made between the values of iron biomarkers in serum of 63 MND patients and those in 53 HCserum. The level of transferrin was similar in patients and HCserum, while a statistically significant difference was found for **ferritin** (p = 0.009, Z = -44.4) and **GPX4** (p = 0.001, Z = -0.835).

Using linear regression analysis within the group of MND patients, I found that transferrin, ferritin and GPX4 levels were not related to genetic profile, severity disease (ALSFRS scale and King’s stage,), or any specific phenotype, including cognitive status. However, a positive correlation (p = 0.006, r = 0.432) was detected between **GPX4** and **PUMNS score** (i.e., a clinical measure of the upper motor impairment); such correlation was found both when considering the total score of PUMNS, as well as when considering the separate scores of bulbar, lower and upper districts (respectively p = 0.004; p = 0.032; p = 0.012). Since iron is naturally

involved in ageing processes, age was also tested as a covariate, and the correlation between GPX4 and PUMNS was confirmed. The duration of disease influences only the levels of transferrin ( $p = 0.044$ ,  $r = -0.261$ ). In the MND group, ferritin and transferrin levels were inversely related to each other ( $p = 0.003$ ,  $r = -0.374$ ), consistently with what is reported in literature. In addition, BMI was found to be correlated with values of transferrin ( $p = 0.025$ ,  $r = 0.294$ ).

### **Correlation among clinical data, iron serum biomarkers and QSM values in MRI**

For the purpose of the following analysis, one patient out of the MND patients with QSM value correctly detected (52), and one subject out of the HCimaging group (24), were excluded as outliers. As previously reported, two types of analysis were performed: by regions of interest (ROIs) and whole brain Voxel-based analysis.

Voxel-based analysis compared MND patients with HCimaging (Figure 2) and detected in ALS patients an increase of susceptibility in **bilateral putamen and left lobule VIII of cerebellum** ( $p < 0.001$  voxel level,  $p < 0.05$  FWE cluster level) and a decrease of susceptibility in **right lobules IV-VI, crus I of cerebellum** ( $p < 0.001$  voxel level,  $p < 0.05$  FWE cluster level).

By comparing MND and HCis, no correlation was found between GPX4 and QSM values. However, when excluding subjects with outlier values of GPX4, a positive correlation was revealed in **right M1** region ( $p < 0.001$  uncorrected voxel,  $p < 0.05$  FWE cluster level) (Figure 3).

In MND group as a result of the ROI analysis, we found a positive correlation: with Gpx4, in **left M1** ( $r = 0.307$ ,  $p = 0.046$ ); with transferrin, in **left PMv** ( $r = 0.346$ ,  $p = 0.026$ ) and **PMd** ( $r = 0.299$ ,  $p = 0.046$ ) and **right SMA** ( $r = 0.321$ ,  $p = 0.041$ ); and with ferritin, in **left lobules IV-V cerebellum** ( $r = 0.034$ ,  $p = 0.032$ ), **caudato** ( $r = 0.0039$ ,  $p = 0.041$ ), **thalamo** ( $r = 0.41$ ,  $p = 0.012$ ), and in **right SMA** ( $r = 0.340$ ,  $p = 0.04$ ). Instead, no significant correlation was found with clinical score of upper motor neuron burden (UPMNS), except for sub-score of PUMNS about upper district in **right preSMA** ( $r = -0.311$ ,  $p = 0.042$ ) and **right SMA** ( $r = -0.337$ ,  $p = 0.027$ ), when the bulbar onset patients were excluded. By performing a trend analysis with rank

of UMN involvement (spinal LMN dominant = 1; spinal = 2; spinal UMN dominant and PLS = 3; bulbar patients were excluded), a positive trend in **left M1** (TJT = 1030,  $p < 0.004$ ) and a negative trend in **left lobules IV-V of cerebellum** (TJT = 221,  $p < 0.032$ ) were identified (Figure 4). The King's stage, that defined the severity of disease at time to visit, did not influence the QSM value.

The Voxel-wise regression analysis across all patients was performed for serum iron biomarker: for GPX4 value (Figure 5), it was revealed an increase of susceptibility in **bilateral precentral gyrus** (in **M1 region**), while for transferrin value (Figure 6) an increase of susceptibility in **right lobules V-VI cerebellum** and a decrease of susceptibility in **left cluster between precentral and postcentral gyrus** (M1 and S1 of ROIs). Instead, no significant variation of susceptibility was revealed examining the Ferritin value.

## **Discussion**

Iron dysregulation is one of the pathogenic mechanisms of MND that promotes oxidative stress and causes progressive loss of motor neurons. In vivo, iron accumulation in cells of brain motor cortex is detected using a specific MRI technique; in addition, in iron-sensitive sequences of MRI, different magnetic susceptibility was found in MND patients classified based on UMN/LMN sign predominance<sup>30,60</sup>. Conversely, ferritin and transferrin, known serum biomarker of iron metabolism in MND, are non-related to any specific phenotype. GPX4 enzyme is one of the key regulators of ferroptosis in nervous cells, as demonstrated in ALS mice models and more recently in pharmacological studies on *Edaravone*, a free radical scavenger tested in ALS.

The main aim of the present study was to explore the correlation between serum iron biomarkers, such as GPX4, ferritin and transferrin, with UMN damage of MND patients and with the QSM values i.e., the in vivo quantification of brain iron accumulation.



First of all, the cohort of MND patients was compared to an age-matched HC group (HCserum) for serum ferritin, transferrin and GPX4 levels.

Results on ferritin and transferrin are consistent with literature findings: ferritin levels were found to be higher in MND, without any specific distribution based on clinical assessment<sup>18</sup>, and the levels of ferritin and transferrin were found to be inversely related to each other. Also, although the correlation between transferrin and BMI of patients has never been previously reported, the result is consistent with the literature findings on the modification of iron homeostasis according to body weight<sup>61</sup>.

Notably, results on GPX4 are a novelty. Indeed, while previous studies on small samples of ALS patients reported that GPX4 was downregulated in spinal cord,<sup>38,39</sup> the present research first shows that serum levels of GPX4 are statistically higher in MND than HC. Serum GPX4 concentration has been previously explored to assess the predictive value of ferroptosis-related biomarker for diabetic kidney disease, and in gestational diabetes mellitus, but no data are available for neurodegenerative diseases.<sup>62,63</sup> Serum GSH level of ALS patients is known to be significantly reduced and GSH synthesis disorders were associated with depletion of GPX4, as showed in mouse models of ALS.<sup>64</sup> The GPX4-knockout mice also showed a like Alzheimer Disease (AD) hippocampal degeneration and an increased levels of marker of ferroptosis such as lipid peroxidation (LPO). In addition, in studies to identify possible candidate of treating for AD, *Edaravone* was chosen for its contribution to ferroptosis restriction by GPX4 and GSH while reducing Fe<sup>2+</sup> and MDA in Abeta 1-42 induced cells<sup>64</sup>. A study engaging different neurodegenerative diseases (AD, Parkinson disease and ALS) will be useful to show the trend of GPX4 levels in serum and, even more interesting, in cerebrospinal fluid.

The subsequent analyses of trend of GPX4 in our cohort of MND did not find any correlation with features of disease, with the exception for the Upper motor neuron burden. In fact, we reported a positive correlation between GPX4 and the presence of Upper motor neuron signs quantified with the PUMNS clinical score for the 3 district (bulbar, upper limbs and lower limbs) considered individually and in total

score. As expected, regardless of duration of disease, patients show higher value of total PUMNS score when in later stages of disease classified with King's stage measuring the number of regions affected by disease ( $p=0,049$ ). Conversely, GPX4 did not significantly change in different stages of disease, suggesting that the role of GPX4 is specific to upper motor neuron damage. Such finding needs to be confirmed in a larger cohort of patients with exclusive involvement of UMN or lower motor neuron. However, we also discovered a positive correlation between levels of GPX4 and the QSM value in a specific motor area (M1), verified with both ROI and Voxel-based analyses. Such outcome, which has never been reported in literature, supports the assumption that the GPX4 is linked to the iron accumulation in brain. The primary motor cortex area (M1) appears to be related to GPX4, both when considering the MND group as well as when comparing MND with HCis (though it should be acknowledged that the number of controls in HCis is limited, and the outcome should be tested against a larger cohort).

For Costagli et al., the diagnostic accuracy of the QSM value in M1 is such as to support clinical examination in the diagnosis of ALS.<sup>65</sup> In addition, the magnetic susceptibility in the precentral cortex could reflect the predominance of upper or lower motor neuron signs in ALS phenotype<sup>32</sup> and the QSM of precentral gyrus could be a support for diagnosis in differentiating UMN of ALS from ALS-mimic subjects.<sup>66</sup> Similarly, in our cohort of MND, a positive trend of QSM was shown with the degree of UMN involvement, from patients with LMN dominant spinal phenotype to PLS and UMN dominant phenotype, in left M1 region. Instead, the supplementary motor area (SMA) and the preSMA on the right side were related to the clinical scale of UMN burden on upper district (PUMNS upper).

To my knowledge, no study has ever verified whether blood measurement in ferritin and transferrin correspond to an increased brain magnetic susceptibility. In this regard, I found that the correlation between these serum iron markers and QSM values was present in known motor regions, as premotor cortex and supplementary motor area, but also in basal ganglia and in cerebellar lobules. Currently, it is not possible to conclude whether this result is a consequence of a correlation with

specific clinical extra-motor signs in MND patients (in particular parkinsonism symptoms<sup>67</sup>) or whether it reflects a widespread accumulation of iron throughout the brain. Moreover, while other whole brain QSM studies identified increased iron in regions including basal ganglia<sup>27</sup>, in our MND cohort we also found changes in susceptibility in cerebellar lobules. This aspect is also worth further investigations for a confirmation of such findings and, eventually, to explore the possible clinical implications.

Another interesting point, not evaluated in the present study, is the longitudinal examination of changes in serum iron biomarkers and in radiological features during the disease progression. However, only one study reported a follow-up of 6-month brain MRI and found no significant changes in QSM.<sup>31</sup> I believe, however, that it would be interesting to measure at least serum levels of GPX4 over time during follow up visits to verify the correlation with the damage of upper motor neuron and the possible predictive value of the enzyme. In this regard, it is not yet known whether MND therapies, such as *Edaravone* or *Riluzole*, can impact on the serum concentration of GPX4.

### **Limitations**

The present study is not without limitations. Although the cohort of patients recruited is representative of ALS patients, it is small in size: a study with a larger population with exclusive involvement of UMN or LMN would be needed to confirm the results. Also, the number of healthy controls with both serum biomarkers and QSM values extracted by brain MRI should be increased.

As reported in the discussion paragraph, while the results suggest that the role of GPX4 is specific to upper motor neuron damage, I have not performed a comparison between groups of patients with different neurodegenerative diseases (AD, PD and FTD), so it cannot be claimed that GPX4 is specific for ALS.

## **Conclusion**

The study explored, in a cohort of 68 MND patients, the role of serum iron biomarkers related to clinical and radiological features by analysing the correlation with UMN the damage. Compared to age-matched healthy controls, I could confirm the higher level of serum ferritin in MND patients that did not correlate with any specific phenotype. In 52 patients, Quantitative Susceptibility Mapping on MRI technique allowed detecting in vivo brain iron accumulation. I therefore correlated the levels of ferritin, transferrin and Gpx4 with the QSM values in motor and premotor cortex area, basal ganglia and cerebellar lobules, in MND patients and HC.

Consistently with the literature findings, in our cohort of MND I found a positive trend of magnetic susceptibility in motor cortex area (M1) with a degree of UMN involvement.

The most relevant result has been the possible role of GPX4 as iron biomarker in serum of MND patients: indeed, I found a significantly higher level of such enzyme in MND patients as compared to HC and, notably, a correlation with the clinical scale of UMN burden. Moreover, I discovered a positive correlation between levels of GPX4 and the QSM value in M1 area.

These findings suggest that GPX4 could be a useful biomarker of UMN involvement in MND patients, linked to iron brain accumulation, with a potential impact on phenotypes differentiation and disease progression prediction.

## Figures

Figure 1. ROIs considered for the motor system (left) and representative Map of QSM in a HCimaging subject (right).

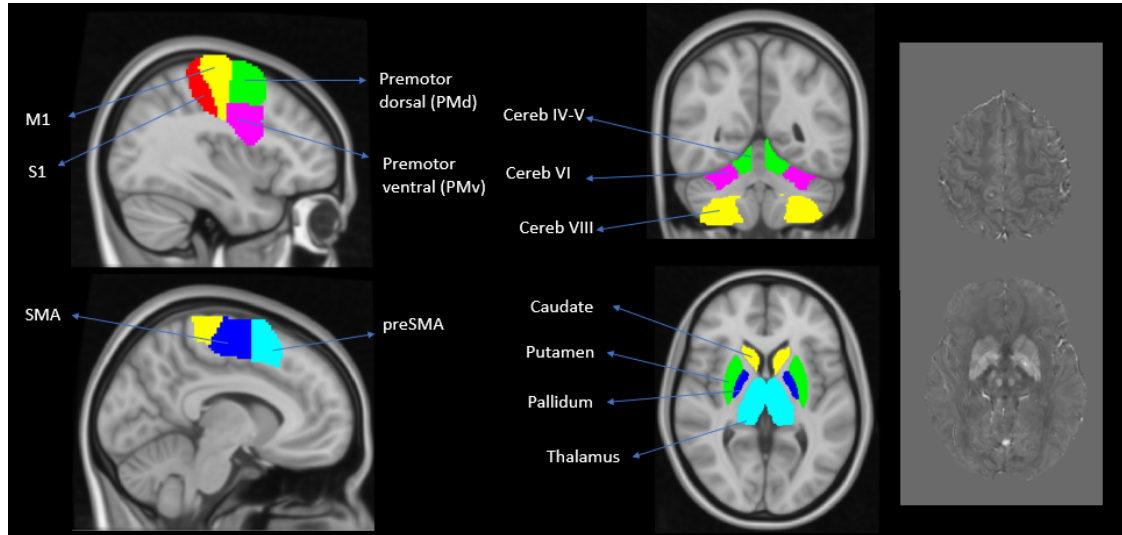


Figure 2. Voxel-wise regression analysis of MND compared to HCimaging.

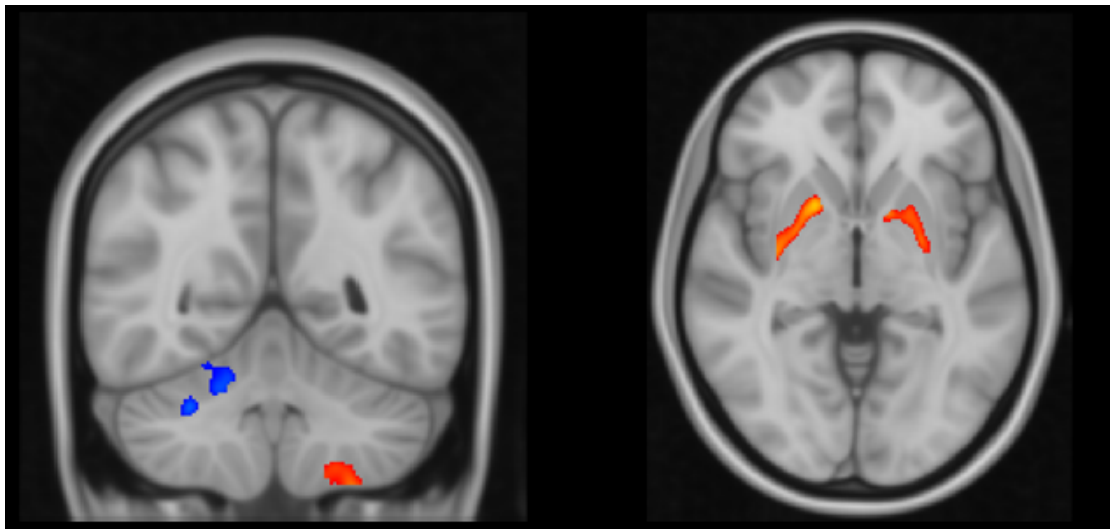


Figure 3. The Voxel-wise regression analysis of MND compared to HCIs to detect a correlation between GPX4 and QSM values.

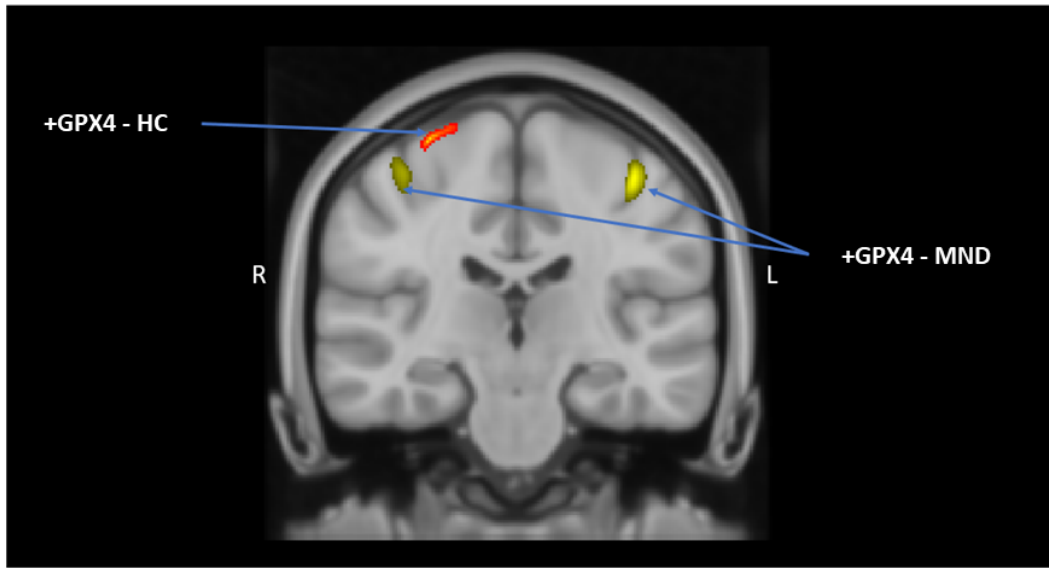


Figure 4. ROI trend analysis with rank in left M1 area (left) and left IV-V lobules of cerebellum (right).

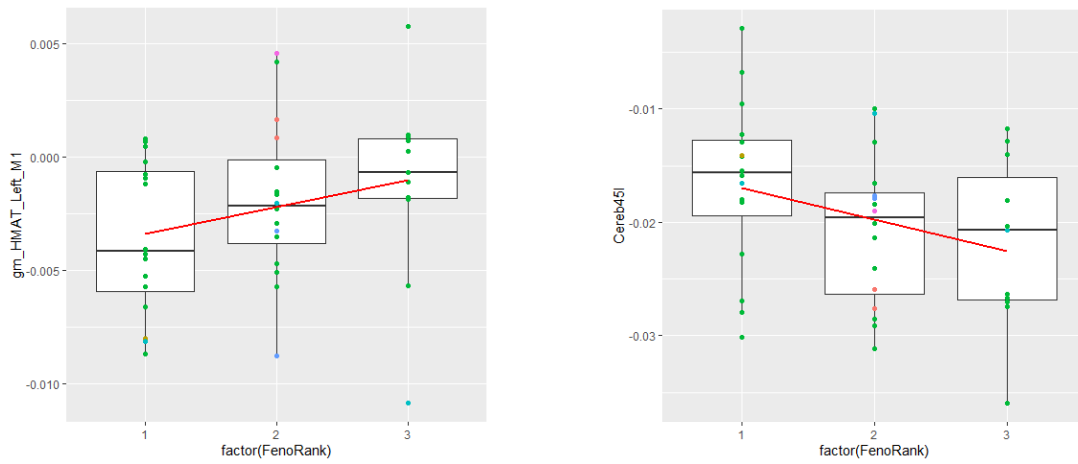


Figure 5. Voxel-wise regression analysis across all MND patients with GPX4 value.

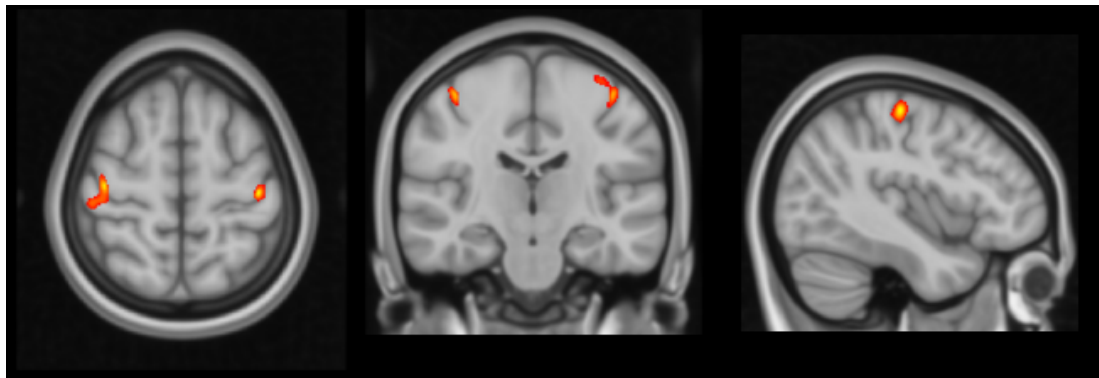
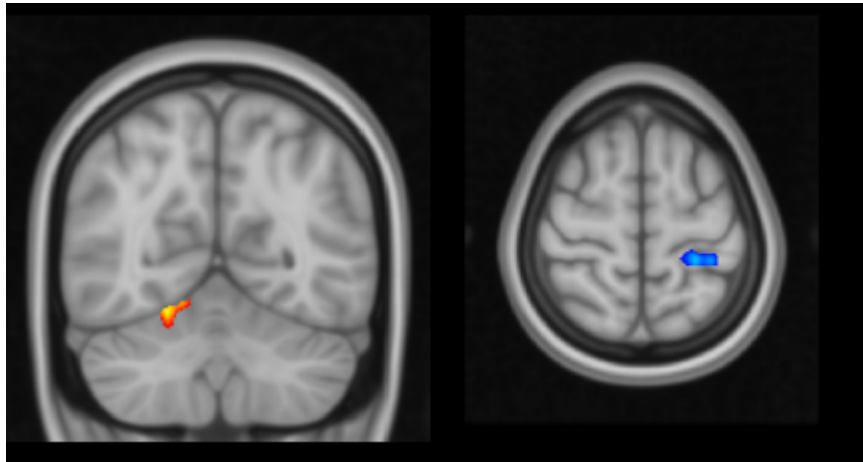


Figure 6. Voxel-wise regression analysis across MND patients with Transferrin value.



## **References**

1. Hardiman O, Al-Chalabi A, Chio A, et al. Amyotrophic lateral sclerosis. *Nat Rev Dis Primers*. Oct 2017;3:17085. doi:10.1038/nrdp.2017.85
2. Andersen PM, Abrahams S, Borasio GD, et al. EFNS guidelines on the clinical management of amyotrophic lateral sclerosis (MALS)--revised report of an EFNS task force. *Eur J Neurol*. Mar 2012;19(3):360-75. doi:10.1111/j.1468-1331.2011.03501.x
3. Goutman SA, Hardiman O, Al-Chalabi A, et al. Recent advances in the diagnosis and prognosis of amyotrophic lateral sclerosis. *Lancet Neurol*. May 2022;21(5):480-493. doi:10.1016/S1474-4422(21)00465-8
4. Verber N, Shaw PJ. Biomarkers in amyotrophic lateral sclerosis: a review of new developments. *Curr Opin Neurol*. Oct 2020;33(5):662-668. doi:10.1097/WCO.0000000000000854
5. Bendotti C, Bonetto V, Pupillo E, et al. Focus on the heterogeneity of amyotrophic lateral sclerosis. *Amyotroph Lateral Scler Frontotemporal Degener*. Jun 2020:1-11. doi:10.1080/21678421.2020.1779298
6. Fang T, Je G, Pacut P, Keyhanian K, Gao J, Ghasemi M. Gene Therapy in Amyotrophic Lateral Sclerosis. *Cells*. Jun 29 2022;11(13)doi:10.3390/cells11132066
7. Ward RJ, Zucca FA, Duyn JH, Crichton RR, Zecca L. The role of iron in brain ageing and neurodegenerative disorders. *Lancet Neurol*. Oct 2014;13(10):1045-60. doi:10.1016/S1474-4422(14)70117-6
8. Nandar W, Neely EB, Simmons Z, Connor JR. H63D HFE genotype accelerates disease progression in animal models of amyotrophic lateral sclerosis. *Biochim Biophys Acta*. Dec 2014;1842(12 Pt A):2413-26. doi:10.1016/j.bbadis.2014.09.016
9. Sutedja NA, Sinke RJ, Van Vught PW, et al. The association between H63D mutations in HFE and amyotrophic lateral sclerosis in a Dutch population. *Arch Neurol*. Jan 2007;64(1):63-7. doi:10.1001/archneur.64.1.63
10. Li M, Wang L, Wang W, Qi XL, Tang ZY. Mutations in the HFE gene and sporadic amyotrophic lateral sclerosis risk: a meta-analysis of observational studies. *Braz J Med Biol Res*. Feb 2014;47(3):215-22. doi:10.1590/1414-431X20133296
11. van Rheenen W, Diekstra FP, van Doormaal PT, et al. H63D polymorphism in HFE is not associated with amyotrophic lateral sclerosis. *Neurobiol Aging*. May 2013;34(5):1517.e5-7. doi:10.1016/j.neurobiolaging.2012.07.020
12. Chiò A, Mora G, Sabatelli M, et al. HFE p.H63D polymorphism does not influence ALS phenotype and survival. *Neurobiol Aging*. Oct 2015;36(10):2906.e7-11. doi:10.1016/j.neurobiolaging.2015.06.016



13. Halon-Golabek M, Borkowska A, Herman-Antosiewicz A, Antosiewicz J. Iron Metabolism of the Skeletal Muscle and Neurodegeneration. *Front Neurosci.* 2019;13:165. doi:10.3389/fnins.2019.00165
14. Kasarskis EJ, Tandon L, Lovell MA, Ehmann WD. Aluminum, calcium, and iron in the spinal cord of patients with sporadic amyotrophic lateral sclerosis using laser microprobe mass spectroscopy: a preliminary study. *J Neurol Sci.* Jun 1995;130(2):203-8. doi:10.1016/0022-510x(95)00037-3
15. Moreau C, Danel V, Devedjian JC, et al. Could Conservative Iron Chelation Lead to Neuroprotection in Amyotrophic Lateral Sclerosis? *Antioxid Redox Signal.* 09 10 2018;29(8):742-748. doi:10.1089/ars.2017.7493
16. Jeong SY, Rathore KI, Schulz K, Ponka P, Arosio P, David S. Dysregulation of iron homeostasis in the CNS contributes to disease progression in a mouse model of amyotrophic lateral sclerosis. *J Neurosci.* Jan 21 2009;29(3):610-9. doi:10.1523/JNEUROSCI.5443-08.2009
17. Winkler EA, Sengillo JD, Sagare AP, et al. Blood-spinal cord barrier disruption contributes to early motor-neuron degeneration in ALS-model mice. *Proc Natl Acad Sci U S A.* Mar 18 2014;111(11):E1035-42. doi:10.1073/pnas.1401595111
18. Wang L, Li C, Chen X, Li S, Shang H. Abnormal Serum Iron-Status Indicator Changes in Amyotrophic Lateral Sclerosis (ALS) Patients: A Meta-Analysis. *Front Neurol.* 2020;11:380. doi:10.3389/fneur.2020.00380
19. Nadjar Y, Gordon P, Corcia P, et al. Elevated serum ferritin is associated with reduced survival in amyotrophic lateral sclerosis. *PLoS One.* 2012;7(9):e45034. doi:10.1371/journal.pone.0045034
20. Agosta F, Spinelli EG, Filippi M. Neuroimaging in amyotrophic lateral sclerosis: current and emerging uses. *Expert Rev Neurother.* 05 2018;18(5):395-406. doi:10.1080/14737175.2018.1463160
21. Bhattarai A, Egan GF, Talman P, Chua P, Chen Z. Magnetic Resonance Iron Imaging in Amyotrophic Lateral Sclerosis. *J Magn Reson Imaging.* Feb 15 2021;doi:10.1002/jmri.27530
22. Kwan JY, Jeong SY, Van Gelderen P, et al. Iron accumulation in deep cortical layers accounts for MRI signal abnormalities in ALS: correlating 7 tesla MRI and pathology. *PLoS One.* 2012;7(4):e35241. doi:10.1371/journal.pone.0035241
23. Yu J, Qi F, Wang N, et al. Increased iron level in motor cortex of amyotrophic lateral sclerosis patients: an in vivo MR study. *Amyotroph Lateral Scler Frontotemporal Degener.* Sep 2014;15(5-6):357-61. doi:10.3109/21678421.2014.906618
24. Adachi Y, Sato N, Saito Y, et al. Usefulness of SWI for the Detection of Iron in the Motor Cortex in Amyotrophic Lateral Sclerosis. *J Neuroimaging.* 2015;25(3):443-51. doi:10.1111/jon.12127

25. Endo H, Sekiguchi K, Shimada H, et al. Low signal intensity in motor cortex on susceptibility-weighted MR imaging is correlated with clinical signs of amyotrophic lateral sclerosis: a pilot study. *J Neurol*. Mar 2018;265(3):552-561. doi:10.1007/s00415-017-8728-0
26. Prell T, Hartung V, Tietz F, et al. Susceptibility-weighted imaging provides insight into white matter damage in amyotrophic lateral sclerosis. *PLoS One*. 2015;10(6):e0131114. doi:10.1371/journal.pone.0131114
27. Acosta-Cabronero J, Machts J, Schreiber S, et al. Quantitative Susceptibility MRI to Detect Brain Iron in Amyotrophic Lateral Sclerosis. *Radiology*. 10 2018;289(1):195-203. doi:10.1148/radiol.2018180112
28. Welton T, Maller JJ, Lebel RM, Tan ET, Rowe DB, Grieve SM. Diffusion kurtosis and quantitative susceptibility mapping MRI are sensitive to structural abnormalities in amyotrophic lateral sclerosis. *Neuroimage Clin*. 2019;24:101953. doi:10.1016/j.nicl.2019.101953
29. Schweitzer AD, Liu T, Gupta A, et al. Quantitative susceptibility mapping of the motor cortex in amyotrophic lateral sclerosis and primary lateral sclerosis. *AJR Am J Roentgenol*. May 2015;204(5):1086-92. doi:10.2214/AJR.14.13459
30. Donatelli G, Caldarazzo Ienco E, Costagli M, et al. MRI cortical feature of bulbar impairment in patients with amyotrophic lateral sclerosis. *Neuroimage Clin*. 2019;24:101934. doi:10.1016/j.nicl.2019.101934
31. Bhattarai A, Chen Z, Ward PGD, et al. Serial assessment of iron in the motor cortex in limb-onset amyotrophic lateral sclerosis using quantitative susceptibility mapping. *Quant Imaging Med Surg*. Jul 2020;10(7):1465-1476. doi:10.21037/qims-20-187
32. Conte G, Contarino VE, Casale S, et al. Amyotrophic lateral sclerosis phenotypes significantly differ in terms of magnetic susceptibility properties of the precentral cortex. *Eur Radiol*. Jul 2021;31(7):5272-5280. doi:10.1007/s00330-020-07547-5
33. Weaver K, Skouta R. The Selenoprotein Glutathione Peroxidase 4: From Molecular Mechanisms to Novel Therapeutic Opportunities. *Biomedicines*. Apr 13 2022;10(4)doi:10.3390/biomedicines10040891
34. Dixon SJ, Lemberg KM, Lamprecht MR, et al. Ferroptosis: an iron-dependent form of nonapoptotic cell death. *Cell*. May 25 2012;149(5):1060-72. doi:10.1016/j.cell.2012.03.042
35. Yang WS, SriRamaratnam R, Welsch ME, et al. Regulation of ferroptotic cancer cell death by GPX4. *Cell*. Jan 16 2014;156(1-2):317-331. doi:10.1016/j.cell.2013.12.010
36. Chen L, Hambright WS, Na R, Ran Q. Ablation of the Ferroptosis Inhibitor Glutathione Peroxidase 4 in Neurons Results in Rapid Motor Neuron Degeneration and Paralysis. *J Biol Chem*. Nov 20 2015;290(47):28097-28106. doi:10.1074/jbc.M115.680090
37. Chen L, Na R, Danae McLane K, et al. Overexpression of ferroptosis defense enzyme Gpx4 retards motor neuron disease of SOD1G93A mice. *Sci Rep*. 06 18 2021;11(1):12890. doi:10.1038/s41598-021-92369-8

38. Wang T, Tomas D, Perera ND, et al. Ferroptosis mediates selective motor neuron death in amyotrophic lateral sclerosis. *Cell Death Differ*. Dec 02 2021;doi:10.1038/s41418-021-00910-z
39. Tu LF, Zhang TZ, Zhou YF, et al. GPX4 deficiency-dependent phospholipid peroxidation drives motor deficits of ALS. *J Adv Res*. Jan 2023;43:205-218. doi:10.1016/j.jare.2022.02.016
40. Zhao K, Li GZ, Nie LY, Ye XM, Zhu GY. Edaravone for Acute Ischemic Stroke: A Systematic Review and Meta-analysis. *Clin Ther*. Dec 2022;44(12):e29-e38. doi:10.1016/j.clinthera.2022.11.005
41. Fidalgo M, Ricardo Pires J, Viseu I, et al. Edaravone for acute ischemic stroke - Systematic review with meta-analysis. *Clin Neurol Neurosurg*. Aug 2022;219:107299. doi:10.1016/j.clineuro.2022.107299
42. Yoshino H. Edaravone for the treatment of amyotrophic lateral sclerosis. *Expert Rev Neurother*. Mar 2019;19(3):185-193. doi:10.1080/14737175.2019.1581610
43. Spasić S, Nikolić-Kokić A, Miletić S, et al. Edaravone May Prevent Ferroptosis in ALS. *Curr Drug Targets*. 2020;21(8):776-780. doi:10.2174/1389450121666200220123305
44. Dang R, Wang M, Li X, et al. Edaravone ameliorates depressive and anxiety-like behaviors via Sirt1/Nrf2/HO-1/Gpx4 pathway. *J Neuroinflammation*. Feb 07 2022;19(1):41. doi:10.1186/s12974-022-02400-6
45. Pang Y, Liu X, Wang X, et al. Edaravone Modulates Neuronal GPX4/ACSL4/5-LOX to Promote Recovery After Spinal Cord Injury. *Front Cell Dev Biol*. 2022;10:849854. doi:10.3389/fcell.2022.849854
46. Brooks BR, Miller RG, Swash M, Munsat TL, Diseases WFoNRGoMN. El Escorial revisited: revised criteria for the diagnosis of amyotrophic lateral sclerosis. *Amyotroph Lateral Scler Other Motor Neuron Disord*. Dec 2000;1(5):293-9. doi:10.1080/146608200300079536
47. Strong MJ, Abrahams S, Goldstein LH, et al. Amyotrophic lateral sclerosis - frontotemporal spectrum disorder (ALS-FTSD): Revised diagnostic criteria. *Amyotroph Lateral Scler Frontotemporal Degener*. 05 2017;18(3-4):153-174. doi:10.1080/21678421.2016.1267768
48. Bakker LA, Schröder CD, Tan HHG, et al. Development and assessment of the inter-rater and intra-rater reproducibility of a self-administration version of the ALSFRS-R. *J Neurol Neurosurg Psychiatry*. Jan 2020;91(1):75-81. doi:10.1136/jnnp-2019-321138
49. Czaplinski A, Yen AA, Appel SH. Forced vital capacity (FVC) as an indicator of survival and disease progression in an ALS clinic population. *J Neurol Neurosurg Psychiatry*. Mar 2006;77(3):390-2. doi:10.1136/jnnp.2005.072660
50. Balendra R, Jones A, Jivraj N, et al. Estimating clinical stage of amyotrophic lateral sclerosis from the ALS Functional Rating Scale. *Amyotroph Lateral Scler Frontotemporal Degener*. Jun 2014;15(3-4):279-84. doi:10.3109/21678421.2014.897357

51. Turner MR, Barohn RJ, Corcia P, et al. Primary lateral sclerosis: consensus diagnostic criteria. *J Neurol Neurosurg Psychiatry*. Apr 2020;91(4):373-377. doi:10.1136/jnnp-2019-322541
52. Quinn C, Edmundson C, Dahodwala N, Elman L. Reliable and efficient scale to assess upper motor neuron disease burden in amyotrophic lateral sclerosis. *Muscle Nerve*. 04 2020;61(4):508-511. doi:10.1002/mus.26764
53. Lancione M, Bosco P, Costagli M, et al. Multi-centre and multi-vendor reproducibility of a standardized protocol for quantitative susceptibility Mapping of the human brain at 3T. *Phys Med*. Nov 2022;103:37-45. doi:10.1016/j.ejmp.2022.09.012
54. Özbay PS, Rossi C, Kocian R, et al. Effect of respiratory hyperoxic challenge on magnetic susceptibility in human brain assessed by quantitative susceptibility mapping (QSM). *NMR Biomed*. Dec 2015;28(12):1688-96. doi:10.1002/nbm.3433
55. Avants BB, Tustison NJ, Song G, Cook PA, Klein A, Gee JC. A reproducible evaluation of ANTs similarity metric performance in brain image registration. *Neuroimage*. Feb 01 2011;54(3):2033-44. doi:10.1016/j.neuroimage.2010.09.025
56. Makris N, Papadimitriou GM, Sorg S, Kennedy DN, Caviness VS, Pandya DN. The occipitofrontal fascicle in humans: a quantitative, in vivo, DT-MRI study. *Neuroimage*. Oct 01 2007;37(4):1100-11. doi:10.1016/j.neuroimage.2007.05.042
57. Mayka MA, Corcos DM, Leurgans SE, Vaillancourt DE. Three-dimensional locations and boundaries of motor and premotor cortices as defined by functional brain imaging: a meta-analysis. *Neuroimage*. Jul 15 2006;31(4):1453-74. doi:10.1016/j.neuroimage.2006.02.004
58. King M, Hernandez-Castillo CR, Poldrack RA, Ivry RB, Diedrichsen J. Functional boundaries in the human cerebellum revealed by a multi-domain task battery. *Nat Neurosci*. Aug 2019;22(8):1371-1378. doi:10.1038/s41593-019-0436-x
59. Stoodley CJ, Schmahmann JD. Functional topography in the human cerebellum: a meta-analysis of neuroimaging studies. *Neuroimage*. Jan 15 2009;44(2):489-501. doi:10.1016/j.neuroimage.2008.08.039
60. Conte G, Sbaraini S, Morelli C, et al. A susceptibility-weighted imaging qualitative score of the motor cortex may be a useful tool for distinguishing clinical phenotypes in amyotrophic lateral sclerosis. *Eur Radiol*. Mar 2021;31(3):1281-1289. doi:10.1007/s00330-020-07239-0
61. Teng IC, Tseng SH, Aulia B, Shih CK, Bai CH, Chang JS. Can diet-induced weight loss improve iron homeostasis in patients with obesity: A systematic review and meta-analysis. *Obes Rev*. Dec 2020;21(12):e13080. doi:10.1111/obr.13080
62. Wu Y, Sun Y, Zhang K, Chen Y. Predictive value of ferroptosis-related biomarkers for diabetic kidney disease: a prospective observational study. *Acta Diabetol*. Apr 2023;60(4):507-516. doi:10.1007/s00592-022-02028-1
63. Zhang B, Zhang T, Hu S, Sun L. Association of serum lipid peroxidation and glutathione peroxidase 4 levels with clinical outcomes and metabolic abnormalities among patients with

gestational diabetes mellitus: a case-control study in the Chinese population. *Front Biosci (Landmark Ed)*. Feb 16 2022;27(2):68. doi:10.31083/j.fbl2702068

64. Wang Y, Lv MN, Zhao WJ. Research on Ferroptosis as a Therapeutic Target for the Treatment of Neurodegenerative Diseases. *Ageing Res Rev*. Aug 22 2023:102035. doi:10.1016/j.arr.2023.102035

65. Costagli M, Donatelli G, Cecchi P, et al. Distribution Indices of Magnetic Susceptibility Values in the Primary Motor Cortex Enable to Classify Patients with Amyotrophic Lateral Sclerosis. *Brain Sci*. Jul 18 2022;12(7)doi:10.3390/brainsci12070942

66. Lo Russo F, Contarino VE, Conte G, et al. Amyotrophic lateral sclerosis with upper motor neuron predominance: diagnostic accuracy of qualitative and quantitative susceptibility metrics in the precentral gyrus. *Eur Radiol*. Aug 22 2023;doi:10.1007/s00330-023-10070-y

67. Balma and Giancarlo Castellano and Marco Barberis and Angelina Cistaro and Carlo Alberto Artusi and Rosario Vasta and Elisa Montanaro and Alberto Romagnolo and Barbara Iazzolino and Antonio Canosa and Giovanna Carrara and Consuelo Valentini and Tie Qiang Li and Flavio Nobili and Leonardo Lopiano and Mario, G. Rizzone ACaACaMPaSCaFDaCMaLSaUMaTMaMBaM. Parkinsonian traits in amyotrophic lateral sclerosis (ALS): a prospective population-based study. *Journal of Neurology*. 2019;266:1633-1642. doi:10.1007/s00415-019-09305-0